湖南大学学报（自然科学版） 第 50 卷 第 7 期
Journal of Hunan University (Natural Sciences) 2023 年 7 月

Available online at http://jonuns.com/index.php/journal/index

Vol. 50 No. 7
July 2023

Open Access Article https://doi.org/10.55463/issn.1674-2974.50.7.6

Identification of Anti-SARS-CoV-2 of *Phyllantus Niruri*, *Curcuma Xanthorrhiza*, and *Orthosiphon Aristatus* Secondary Metabolites through *In Silico* Studies

Ruth Ellen[1], Sri Fatmawati[1,2]*, Arli Aditya Parikesit[3]

[1] Department of Chemistry, Faculty of Science and Data Analytics, Institut Teknologi Sepuluh Nopember, Surabaya, East Java, Indonesia

[2] Agri-Food and Biotechnology Research Center, Institut Teknologi Sepuluh Nopember, Surabaya, East Java, Indonesia

[3] Department of Bioinformatics, School of Life Sciences, Indonesia International Institute for Life Sciences, Jakarta, Indonesia

* Corresponding author: fatma@chem.its.ac.id

Received: April 10, 2023 / Revised: May 13, 2023 / Accepted: June 11, 2023 / Published: July 31, 2023

Abstract: SARS-CoV-2 caused a global pandemic in 2019 with mild flu-like clinical symptoms to severe symptoms that can cause death. Research to find the SARS-CoV-2 drug has been carried out through literature and *in silico* studies against SARS-CoV-2. Previous studies have reported the antiviral properties of some Indonesian herbs including *Phyllantus niruri*, *Curcuma xanthorrhiza* and *Orthosiphon aristatus*. However, secondary metabolites from these plants have not been tested for anti-SARS-CoV-2. Therefore, the aim of this study is to reveal the anti-SARS-CoV-2 activity of secondary metabolites of these plants through *in silico* study. Molecular docking and molecular dynamic simulation of compounds were tested using Autodock Vina and GROMACSS 2021.2 against spike (S) glycoprotein and 3-chymotrypsin-like protease ($3CL^{pro}$) as drug target. Further, the potential SARS-CoV-2 drugs were analyzed for drug similarity and Absorption, Distribution, Metabolism, Excretion and Toxicity (ADMET) properties. The results exhibited that rutin (-7.3 kcal/mol), ellagic acid (-7.2 kcal/mol) and ursolic acid (-6.8 kcal/mol) has better docking score for S-glycoprotein than nelfinavir (-6.7 kcal/mol) and remdesivir (-6.6 kcal/mol). In addition, rutin (-8.8 kcal/mol) had a better docking score for $3CL^{pro}$ than nelfinavir (-8.2 kcal/mol) and remdesivir (-7.8 kcal/mol). It could bind to S-glycoprotein and $3CL^{pro}$ binding receptor domain. Molecular dynamics simulations showed stable $3CL^{pro}$-rutin complex. The ADMET properties of rutin showed it is non-toxic. Therefore, rutin is a good $3CL^{pro}$ inhibitor and has the potential to be a SARS-CoV-2 drug.

Keywords: SARS-CoV-2, *in silico*, *Phyllantus niruri*, *Curcuma xanthorrhiza*, *Orthosiphon aristatus*.

通过计算机模拟研究鉴定叶下珠、姜黄和 正虹吸虫 次级代谢物的抗 SARS-CoV-2

摘要：SARS-CoV-2 在 2019 年引起了全球大流行， 其临床症状类似于轻微的流感样临床症状，严重的症状可能导致死亡。寻找 SARS-CoV-2 药物的研究是通过文献和针对 SARS-CoV-2 的计算机模拟研究进行的。先前的研究报道了一些印度尼西亚草药的抗病毒特性，包括叶下珠、姜黄和直虹吸虫。然而，这些植物的次生代谢物尚未经过抗 SARS-CoV-2 测试。因此，本研究的目的是通过计算机模拟研究揭示这些植物次生代谢产物的抗 SARS-CoV-2 活性。使用维纳奥托克和格罗玛斯 2021.2 针对刺突(S)糖蛋白和 3-胰凝乳蛋白酶样蛋

白酶(3CLpro)作为药物靶标，测试了化合物的分子对接和分子动力学模拟。此外，还分析了潜在的 SARS-CoV-2 药物的药物相似性以及吸收、分布、代谢、排泄和毒性(阿德梅特)特性。结果表明，芦丁（-7.3 千卡/摩尔）、鞣花酸（-7.2 千卡/摩尔）和熊果酸（-6.8 千卡/摩尔）对 S-糖蛋白的对接分数优于奈非那韦（-6.7 千卡/摩尔）和瑞德西韦（-6.6 千卡/摩尔）。此外，芦丁（-8.8 千卡/摩尔）与 3CLpro 的对接得分优于奈非那韦（-8.2 千卡/摩尔）和瑞德西韦（-7.8 千卡/摩尔）。它可以结合 S-糖蛋白和 3CLpro 结合受体结构域。分子动力学模拟显示稳定的 3CLpro-芦丁复合物。芦丁的阿德梅特特性表明它是无毒的。因此，芦丁是一种良好的 3CLpro 抑制剂，有潜力成为 SARS-CoV-2 药物。

关键词：SARS-CoV-2，计算机模拟，叶下珠、姜黄、直虹吸虫.

1. Introduction

A new variant of the coronavirus, SARS-CoV-2, which causes Corona Virus Disease-19 (COVID-19), was first discovered in the city of Wuhan, Hubei Province, China [1]-[4]. SARS-CoV-2 has become a global pandemic of concern. Data on February 27, 2021, shows that the ratio of COVID-19 sufferers in Indonesia compared to 7.1 million people tested for Polymerase Chain Reaction (PCR) is 18.53%. This is the highest ratio in Southeast Asia [5].

WHO has determined that viruses within the lineage B.1.617, which are B.1.617.1, B.1.617.2 and B.1617.3, as variant of concern in the weekly epidemiological update on May, 11th 2021 [6]. Over time, B.1.617.1 (known as Kappa variant) was demoted as variant of interest as well as Epsilon (B.1.427/B.1.429), Zeta (P.2), Eta (B.1.525), Theta (P.3), Iota (B.1.526) and Lambda (C.37) variants on June 22, 2021. The variants of concern were Alpha (B.1.17), Beta (B.1.351), Gamma (P.1) and Delta (B.1.617.2). The alpha variant has been reported to retain neutralizing activity, while the others have been reported to reduce the neutralizing activity. Beta and gamma increased transmissibility, while alpha and delta variants increased transmissibility and secondary attack [7].

Patients infected with SARS-CoV-2 mild clinical symptoms such as dry cough, sore throat, and fever. Some cases recover spontaneously, but in other cases SARS-CoV-2 results in various fatal complications such as organ failure, septic shock, pulmonary edema, acute pneumonia, and acute respiratory distress syndrome (ARDS). Elderly patients with multiple comorbid factors including cardiovascular, cerebrovascular, endocrine, digestive, and respiratory diseases require intensive care support. These patients are often reported to experience dizziness, abdominal pain, and anorexia [8]. Severe symptoms suffered by patients can lead to death [2].

Based on homology analysis, the SARS-CoV-2 genome is composed of single-stranded RNA. SARS-CoV-2 is included in beta coronavirus along with Bat SARS, SARS-CoV, and MERS-CoV. However, SARS-CoV-2 is similar to SARS-CoV and Bat SARS based on the structure of its genome. Corona viruses have a similar receptor-binding domain. Spike (S) glycoprotein as the binding domain of SARS-CoV-2 is homologous to SARS-CoV by about 75% [1-4, 9].

Coronavirus infects its host in three stages. First, the virus attaches the transmembrance Spike glycoprotein (S-glycoprotein) to the host ACE2. The attachment forms a complex with the help of transmembrance protease serine 2 (TMPRSS2) produced by the host cell. The second stage is viral replication using RNA-dependent RNA polymerase (RdRp) to replicate in host cells. The last stage is the maturation of viral replication using proteases such as $3CL^{pro}$ and PL^{pro}. These three stages are important for developing drug targets against the coronavirus [10]. S-glycoprotein and protein $3CL^{pro}$ were targets of anti-SARS-CoV-2 in this study.

The World Health Organization (WHO) in 2001 estimated that 80% of the population in some Asian and African countries currently use medicinal plants in some aspects of primary health care. This encourages experts in the fields of pharmacology, microbiology, botany and natural products chemistry to search for phytochemical compounds that can be developed for the treatment of diseases. Facts obtained by the WHO indicate that about 25% of modern medicine used in the United States comes from plants. 80% of isolated compounds used in modern medical therapy show a positive correlation between modern medical therapy and the traditional use of compounds [11].

Chemical compounds in plants affect the human body through the same process as conventional medicine. The way herbal medicine works is not much different from conventional medicine. This allows the effectiveness of herbal medicines to be the same as conventional medicines, but the potential to cause harmful side effects to be the same [11]. Based on this, further research is needed regarding the prediction of

drug similarity based on Lipinski's rules (Lipinski, et al, 2012) [12]; properties of Absorption, Distribution, Metabolism, Excretion and Toxicity (ADMET) as well as the right dosage. In addition, it is necessary to perform a quantitative structure activity relationship (QSAR) test in the early stages of the drug discovery process to find compounds that have antiviral activity [13]-[14] that can be used as SARS-CoV-2 inhibitors.

The molecular docking studies of the anti-SARS-CoV-2 ability of several active compounds from Indonesian medicinal plants exhibited that some compounds were known to have lower binding energies to S-glycoprotein and $3CL^{pro}$ than antiviral drugs. The low binding energy indicates the high affinity of phytochemical compounds for S-glycoprotein and $3CL^{pro}$, so the lower the binding energy, the higher the anti-SARS-CoV-2 ability of phytochemical compounds [15]. After the docking score is obtained, the research can be continued with molecular dynamics simulations to determine the resistance of the ligands [16].

During the rapid development of molecular docking studies, many compounds have not been tested for their anti-SARS-CoV-2, including phytochemical compounds contained in meniran (*P. niruri*), temulawak (*C. xanthorriza*), and kumis kucing (*O. aristatus*). The ethanol extract, phyllanthine and hypophilanthine compounds of *P. niruri* showed antiviral activities against Hepatitis C visrus [17]. *P. niruri* has been tested for its antiviral activity against Influenza, Hepatitis B and Human Immunodeficiency (HIV) viruses [18], Herpes Simplex Virus Type I (HSV-1) and Herpes Simplex Virus Type 2 (HSV-2) [19]. *C. xanthorrhiza* extract exhibited antiviral properties against Simian Retrovirus type-2 (SRV-2) [20], while curcuminoids (curcumin, demethoxy curcumin, bisdemethoxy curcumin) as active substances in *C. xanthorrhiza* had antiviral properties [21]. O. aristatus extract was potential to be an anti-HSV-1 and anti-vesicular stomatitis virus (VSV) agent [22,23].

Based on the explanation above, a molecular docking study of the active compounds that have antiviral activity contained in *P. niruri*, *C. xanthorrhiza* and *O. aristatus* would be conducted. The result of molecular docking for high binding affinity with SARS-CoV-2 molecules will be followed by molecular dynamics simulations to determine the resistance of the complex of protein-compound, drug similarity tests based on Lipinski rules and the properties of ADMET to determine the ability and safety of compounds used as drugs.

2. Materials and Methods

2.1. Determination of Ligand

Several secondary metabolites exhibited antiviral activity based on literature studies, were used as ligands in the docking process. These compounds were: rutin (1) and quercetin (2) (flavonoid compounds), phyllantin (3), hypophyllanthin (4) and niruriside (5) (lignan compounds), repandusinic acid (6) and geraniin (7) (tannin compounds), ellagic acid (8) (coumarin group), camphor (9) (an oxygenated monoterpene), germacrone (10) (an oxygenated sesquiterpene compound), curcumin (11) and demethoxycurcumin (12) (curcuminoid compounds), rosmarinic acid (13) (polyphenolic compounds), stigmasta-5,22-dien-3-ol (14), ursolic acid (15) and oleanolic acid (16) (triterpenoids compounds). Compounds 1-8 are found in *P. niruri* leaves, compounds 9-12 are found in *C. xanthorrhiza* roots, and compounds 13-16 are found in *O. aristatus* leaves. The reference standards drugs were Remdesivir and Nelfinavir.

2.2. Protein Preparation

The two selected SARS-CoV-2 drug discovery targets were S-glycoprotein (PDB code: 6LZG) and $3CL^{pro}$ (PDB code: 6LU7). Proteins were prepared using Biovia Discovery Studio. Water molecules were removed and the active sites were determined. Once the active site was known, the protein chain other than the active site was deleted. Polar hydrogen was added and the prepared protein was saved in PDB (Protein Data Bank) format.

2.3. Quantitative Structure Activity (QSAR) Prediction

The first step to predict the suitability of compounds used as anti-SARS-CoV-2 was to determine the antiviral activity through QSAR prediction. QSAR predictions could be accessed on the PASS server (http://www.pharmaexpert.ru/passonline/) [14]. Compounds with $Pa > 0.3$ are declared active [24].

2.4. Molecular Docking

Molecular docking was carried out to predict the affinity of plant-derived antiviral compounds against the SARS-CoV-2 S-glycoprotein and $3CL^{pro}$ using Autodock Vina program. Proteins that had been stored in PDB form were opened using Autodock Vina and given the Kollman charges. The Gasteiger charges were calculated. The protein was saved using the pdbt format. Input the ligand to be tested and saved in pdbt format. The grid was arranged with protein selected as macromolecules and ligand as set map types. The x, y and z grid maps were filled according to the Biovia Discovery Studio active side data and exhaustiveness is set at 8 according to the Autodock Vina default. The Command Prompt program is used to run Autodock Vina. This procedure based on literature with modifications [25].

2.5. Molecular Dynamic Simulation

Molecular dynamics simulations were run based on literature with modifications [25]. The GROMACS-

2021.2 software was used in the atomic molecular dynamics simulation process with all CHARMM36 atomic force fields (February 2021) for the top protein-ligand complexes sorted based on docking score. The ligand topology was generated through the CHARMM General Force Field (CGenFF) program using cgenff_charmm2gmx_py2.py. The protein-ligand complex system was dissolved in a cubic box (size determined by keeping the closest protein atom to the box boundary at 1 nm) of TIP3P (transferable intermolecular potential with 3 points).

The charge of the system was neutralized by adding counter ions. Charge interactions (electrostatic) were calculated by the particle mesh Ewald (PME) method. The 6LU7 protein was neutralized with 4 Na+, and the 6LZG protein was neutralized with 24 Na+. After the purification of the complex with energy minimization, an isothermic-isovolumetric (NvT) simulation and an isobaric-isothermic NpT 100 ps simulation were performed to balance the water box.

Next, another MD simulation was run for 10 ns NpT for simulated production at a constant temperature of 300 K at 1 atm pressure. Anisotropic diagonal position scaling at 0.002 ps time step intervals was used to maintain constant pressure during the MD simulation. The Lennard-Jones and Coulomb short-range interactions energy was calculated on radius 1.2 nm, while the electrostatic calculation for long-range PME with a Grid Fourier distance of 0.16 nm. The Berendsen temperature coupling method (V-rescale) was used to maintain the temperature in the box. The NpT equilibrium was achieved by the Parrinello-Rahman pressure coupling method. The results obtained from this simulation were root mean square deviation (RMSD) and Coulomb and Lennard-Jones short-range energies.

3. Results and Discussion

3.1. QSAR Prediction

The QSAR predictive result of secondary metabolites showed a lot of information about the bioactivity of secondary metabolites tested in this study. The various information was filtered to obtain predictive results regarding the antiviral properties of the tested compounds, both general antiviral properties and antiviral properties against viruses similar to SARS-CoV-2, including picornavirus, rhinovirus and influenza virus. The QSAR result is showed in Table I.

Picornaviruses are small nonenveloped RNA viruses. The genomic RNA consists of 7500–8000 nucleotides. The members of PV are rhinoviruses, enteroviruses, coxsackieviruses, polioviruses, echoviruses, encephalomyocarditis viruses, meningitis virus, foot and mouth viruses, hepatitis A virus, and so on. The picornavirus $3CL^{pro}$ protein is analogous to the SARS-CoV $3CL^{pro}$ [26, 27]. $3CL^{pro}$ protein plays a role in the process of two overlapping polyproteins pp1a (486 kDa) and pp1b (790 kDa), therefore $3CL^{pro}$ plays a role in viral protein maturation [26].

Table 1 QSAR prediction result

Compound	Antivirus		Anti-Influenza		Anti-Rhinovirus		Anti-Picornavirus	
	Pa	Pi	Pa	Pi	Pa	Pi	Pa	Pi
(1)			0.743	0.004				
(2)			0.403	0.046				
(3)			0.293	0.094	0.367	0.133	0.339	0,171
(4)								
(5)	0.221	0.080			0.348	0.163		
(6)	0.248	0.061						
(7)	0.027	0.075	0.438	0.035	0.447	0.051		
(8)	0.322	0.029	0.254	0.138			0.364	0.162
(9)					0.333	0.189	0.393	0.116
(10)							0.417	0.097
(11)	0.418	0.013	0.471	0.028				
(12)	0.412	0.013	0.462	0.030				
(13)	0.305	0.035	0.412	0.043	0.399	0.092	0.327	0.187
(14)			0.506	0.022	0.487	0.029		
(15)			0.761	0.004	0.492	0.027		
(16)	0.242	0.065	0.836	0.002	0.481	0.032		

Notes: Pa - probability active, Pi - probability inactive, Pa > 0,3 is active

Unlike the Coronavirus which is a positive single RNA virus, the influenza virus is a negative single RNA virus with the main antigenic factors being the transmembrane glycoprotein hemagglutinin (HA) and neuraminidase (NA). Despite their differences, these two viral infections have similar clinical symptoms and can cause a cytokine storm in the lung [28].

Compounds (1) and (2), members of flavonoid compounds, are active as anti-influenza virus based on the prediction. Compound (3) is active as anti-rhinovirus and picornavirus. However, the result exhibits no information about (4), a phyllantin derivative, antiviral activity against these viruses. (6) is active as anti-rhinovirus. Compounds (14), (15), (16) are active as anti-influenza and anti-rhinovirus. Compound (8) is predicted to be active as antiviral and

anti-picornavirus. Compound (9) is predicted to be active as anti-rhinovirus and picornavirus, while (10) is predicted to be anti-picornavirus active. Compounds (11) and (12), members of curcuminoid, are active as antiviral and anti-influenza. Compound (13) is predicted to be active in all category. The active compounds were evaluated further for its antiviral activity against SARS-CoV-2.

3.2. Molecular Docking

The molecular docking between compounds with 6LZG protein (receptor binding domain for S-glycoprotein that binds to human ACE2) and 6LU7 ($3CL^{pro}$ structure that binds to natural inhibitors (N3)) was carried out using the Biovia Discovery Studio program for the initial step of protein preparation. Proteins were obtained from the RSCB page in PDB format. Water molecules contained in protein molecules were removed because the water molecules contained in protein-ligand complexes can cause deviations due to the ideal hydrogen bond geometry involving water molecules [29]. The next step is to determine the scope of the Structure-Based Design (SBD) site selected based on the location of the natural ligand at 6LU7 and the location of the viral S-glycoprotein attachment to human ACE2 at 6LZG. After that, chains that were not within the specified site scope were deleted. The addition of polar hydrogen was carried out because ambiguous X-ray crystallographic structures and the loss of polar hydrogen atoms were often encountered [30]. Protein files are saved in PDB form.

The molecular docking was carried out using Autodock Vina program, because this program is equipped with many CPU cores so that the running time required is shorter than Autodock 4.2. In addition, the results of this program are more accurate than the results of Autodock 4.2 [31]. Protein that had been stored in PDB format were opened using Autodock Vina and given a Kollman charge and because the ligand was not a peptide chain it needed Gasteiger charge. In addition, it was important to pre-calculate the grid map [32]. The grid map parameter used was AD4 type. Proteins and ligands were stored in pdbqt format for docking process. Further, grid arrangement was done by selecting proteins as macromolecules and selecting ligands in the set map types setting. The configuration file was set by choosing protein.pdbqt as macromolecules and ligand.pdbqt as ligand. Furthermore, the grid in the configuration file was set according to the scope of the SBD site from Biovia Discovery Studio for accurate results. Molecular docking was done by running the Autodock Vina program via Command Prompt. The docking result is shown in Table II.

Table 2 Molecular docking score of secondary metabolites to S-glycoprotein (6LZG) and $3CL^{pro}$ (6LU7)

Compounds	Score (ΔG kcal/mol)	
	6LZG	**6LU7**
(1)	-7.3	-8.8
(2)	-6.5	-7.4
(3)	-4.5	-6.1
(5)	-6.6	-6.8
(7)	-6.5	-7.2
(8)	-7.2	-7.3
(9)	-4.2	-4.5
(10)	-6.1	-5.5
(11)	-5.8	-7.1
(12)	-6.0	-7.2
(13)	-6.6	-7.1
(14)	-6.5	-7.1
(15)	-6.8	-7.6
(16)	-6.2	-7.7
Remdesivir	-6.7	-7.8
Nelfinavir	-6.6	-8.2

The molecular docking score showed three compounds with the lowest free energy (the best binding score) to 6LZG protein, namely: compounds (1), (8) and (15) with free energy values of -7.3 -7.2 and - 6.8 kcal/mol. The free energy obtained by protein 6LZG-this compound was lower than 6LZG-remdesivir and 6LZG-nelfinavir. Visualization of docking results on the best score was done through the Biovia Discovery Studio program. The results of this visualization showed that oxygens of (1) were conventional hydrogen bond acceptor from ARG403, TYR449, GLN493, GLN498 and a hydrogen bond donor to ASN501. In addition, carbon of (1) was a carbon-hydrogen bond donor to SER494. The pi-cation type electrostatic interaction occured between the positively charged NH group of ARG403 and the pi-orbital of (1). Hydrophobic interactions with aromatic-aromatic interactions (pi-pi stacked) occured between TYR453 and two pi-orbitals of (1) and pi-pi interactions of the T form occurred between TYR505 and pi-orbitals of (1) (Figure 1A).

The visualization of the docking of (8) showed hydrogen bonds and hydrophobic interactions between the S-glycoprotein SARS-CoV-2 and this compound. Conventional hydrogen bonding occurred between the hydrogen ARG403 and the oxygen of (8). In addition, (8) became a hydrogen bond donor to ASN501 and TYR505. Pi-donor type hydrogen bonding occurred between nitrogen GLY496 and the two pi-orbitals of this compound. Hydrophobic interactions of the pi-pi T-shaped occurred between the pi-orbital TYR505 and (8) (Figure 1B). Different results were obtained by (15) which at its best docking score only had conventional hydrogen bonds between the hydrogen of GLY496 and the oxygen of this compound (Figure 1C).

Visualization of S-glycoprotein binding results with reference drugs remdesivir and nelfinavir is shown for comparison. Several oxygen atoms of nelfinavir became hydrogen bond acceptors with ARG403, TYR453, GLN493, and GLY496. The drug's hydrogen atom also acted as a hydrogen bond donor to the oxygen of GLU406. The pi-alkyl hydrophobic interactions occurred between the pi-orbital TYR505

and the alkyl nelfinavir and between the pi-orbital nelfinavir and LYS417 (Figure 1D). Different results were shown by visualization of the 6LZG-remdesivir, in which the interaction between the 6LZG-remdesivir protein complex was only hydrophobic interactions. The pi-sigma hydrophobic interaction occurred between the C-H remdesivir and the pi-orbital TYR489, while the alkyl hydrophobic interaction occurred between the remdesivir alkyl and LEU455. The pi-alkyl hydrophobic interactions occurred between the pi-orbital PHE456 and the two alkyl remdesivir and between the pi-orbital of this drug and the alkyl LYS417 (Figure 1E).

Based on a literature study on the molecular dynamics of the SARS-CoV-2 S-glycoprotein complex with human ACE2, a stable salt bridge was formed between LYS417 of the SARS-CoV-2 protein and ASP30 ACE2 and a stable hydrogen between TYR449, GLN493, and GLN498 of SARS-COV-2 with ASP38, GLU35, and LYS353 of ACE2 [33]. Therefore, it is essential to interfere with the bonding formation between S-glycoprotein and ACE2. Compound (1) might intervene in the formation of the hydrogen compound ACE2-S-glycoprotein in TYR449, GLN493, GLN498, while nelfinavir interfered in GLN493 and the salt bridge LYS417 and remdesivir only interfered in the salt bridge in LYS417. The result showed that (1) is a strong anti-SARS-CoV-2 candidate that can fight against this entry virus by forming a complex with human ACE2.

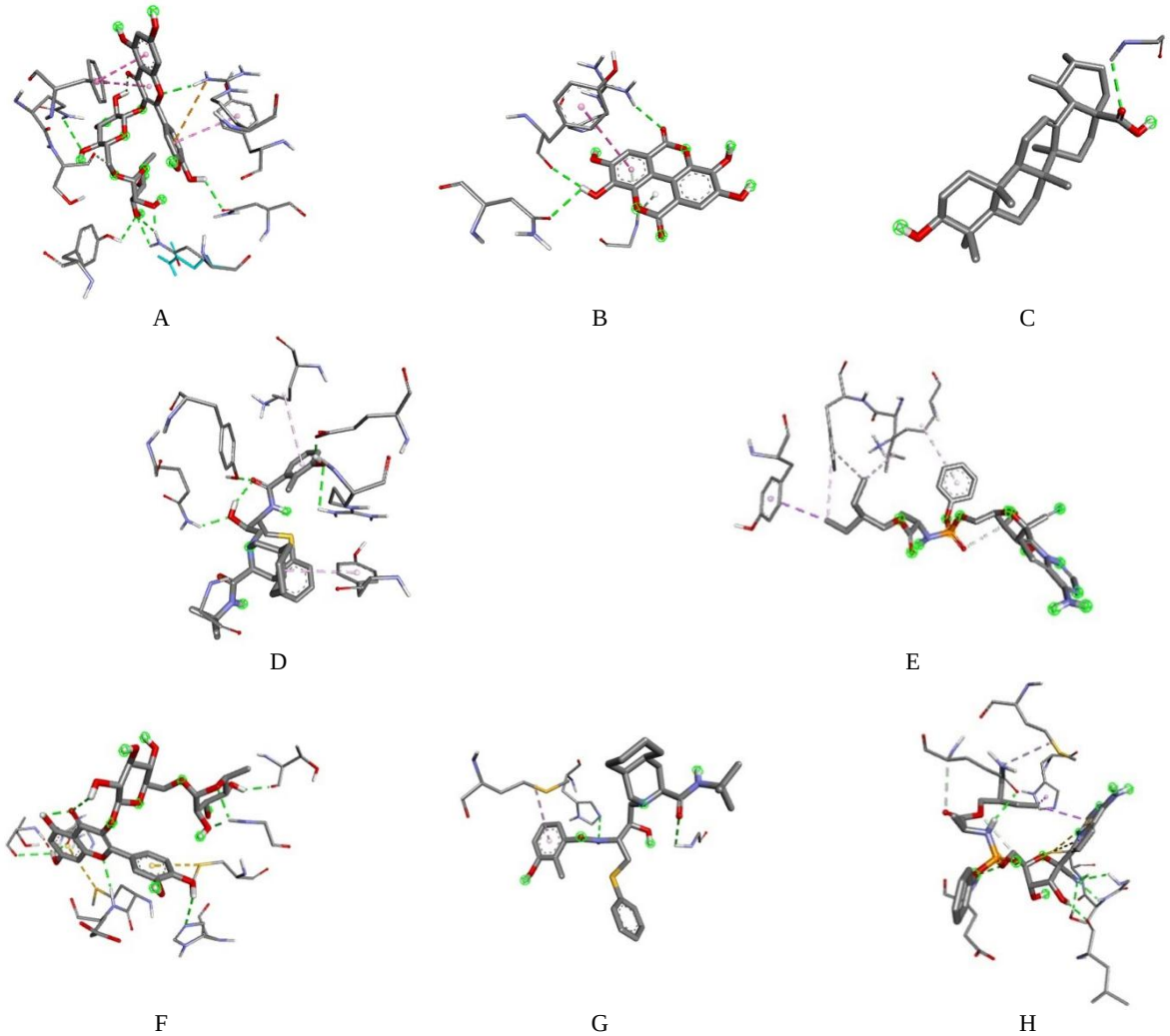

Fig. 1 Molecular docking visualization of *P. niruri*, *C. xanthorrhiza* and *O. aristatus* secondary metabolites and reference drugs: A. 6LZG-(1), B. 6LZG-(8), C. 6LZG-(15), D. 6LZG-nelfinavir, E. 6LZG-remdesivir, F. 6LU7-(1), G. 6LU7-nelfinavir, H. 6LU7-remdesivir

The molecular docking of secondary metabolite compounds with 6LU7 binding score exhibited that the 6LU7-(1) complex had the lowest free energy compared to the 6LU7-remdesivir complex and the 6LU7-nelfinavir complex. Visualization of the docking results on the best score of (1) showed that two oxygen of this compound were hydrogen bond acceptors from GLY143 and one oxygen of (1) was hydrogen bond acceptor from GLU166. (1) also acted as hydrogen bond donor to oxygen THR26, ARG188, THR190 and nitrogen HIS163. In addition, there were pi-sulfur interaction between sulfur CYS145 and MET165 with pi-orbital of (1) (Figure 1F).

Visualization of nelfinavir binding results showed the pi-orbital of this drug interacted hydrophobically with pi-sigma type with ALA292. Pi-alkyl hydrophobic interactions occurred between the pi-orbital PHE318 and the alkyl drug (Figure 1G). Different results were

shown by Remdesivir. Remdesivir interacted electrostatically between its positive and negative charges to GLU298. Hydrogen bonding occurred between remdesivir hydrogen to oxygen ARG319, SER316 and ARG319. Hydrogen bonding with a carbon-hydrogen occurred between remdesivir carbon and CYS291. The pi-sigma type hydrophobic interaction occurred between VAL595 C-H and the pi-orbital of remdesivir. The hydrophobic alkyl-alkyl interaction occurred between the alkyl of CYS291 and the alkyl of remdesivir (Figure 1H).

Literature studies suggest that proteolysis occurs through catalytic dyads, namely CYS145 and HIS41 [34]-[35]. The two catalytic points become binding receptors important for inhibiting viral replication. There were pi-sulfur interactions with CYS145 and interactions with other active binding receptor residues, namely GLY143, GLU166, THR26, ARG188, THR190 and HIS163. Based on this explanation, (1) could be an inhibitor of $3CL^{pro}$ SARS-CoV-2 candidate.

3.3. Molecular Dynamic Simulation

The RMSD results of molecular dynamics simulation for 10 ns showed that the RMSD value of 6LU7-(1) complex fluctuated in a narrow range of 0.95-1.22 nm while the RMSD fluctuation range for bare protein was 0.0005-0.282. These results indicate that the 6LU7-(1) complex was stable during the molecular dynamics simulation. The average RMSD value of 6LU7-(1) complex was 1.037 nm while the average RMSD value of 6LU7 protein without ligand was 0.205. The average RMSD value of the 6LU7-(1) complex was slightly higher than the average RMSD value of the 6LU7 bare protein.

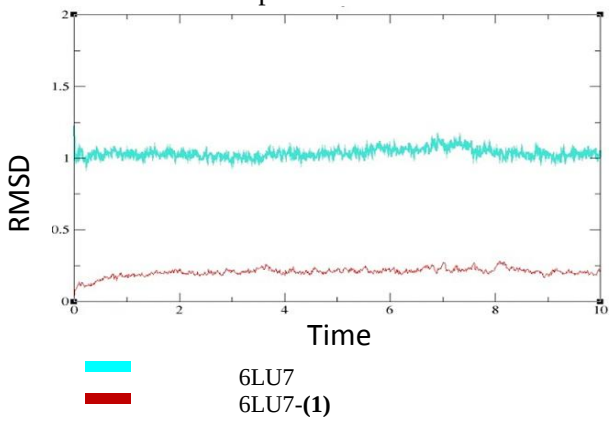

Fig. 2 RMSD of 6LU7 and 6LU7-(1)

The average short-range Coloumb interaction energy of 6LU7-(1) complex was -212.861 ± 5.4 kJ/mol. The average short-range Lennard-Jones interaction energy was -222.114 ± 6.8 kJ/mol. The total interaction energy of 6LU7-(1) complex with error propagation was -434.975 ± 8.68 kJ/mol.

3.4. ADMET Properties

Predictions of drug similarity, ADMET properties, and synthetic accessibility were obtained through Swissadme filters. The pharmacokinetic properties of (1) indicates that this compound is poorly absorbed in the digestive system and can bind to P-glycoprotein (P-gp) which can inhibit drug absorption. P-gp is a transporter that facilitates the secretion of molecules back into the intestinal lumen thereby limiting the absorption [36]. (1) is not an inhibitor of CYP1A2, CYP2C19, CYP2C9, CYP2D6 and CYP3A4 and could not penetrate the blood brain barrier so it is good for use as a drug [37]. The synthetic accessibility score of (1) which is based on fragmental analysis of the structure is 6.31, indicating that (1) is quite easy to synthesize.

However, (1) violates 3 Lipinski's rule of five, including molecular mass more than 500, hydrogen bond acceptor more than 10, and hydrogen bond donor more than 5. This violation is normal. Some very popular drugs, for example dabigatran etexilate, bromocriptine mesylate, olmesartan medoxomil, fosinapril, and reserpine, violate two of Lipinski's rules. Some very popular tyrosine kinase inhibitors (lapatinib and nilotinib) and HIV protease inhibitors (lopinavir, atazanavir, nelfinavir) violates 3 Lipinski's criteria. Atazanavir demonstrated three violations of Lipinski's rule [25]. Even remdesivir violates 2 Lipinski's rules because the molecular mass is more than 500 and the hydrogen bond acceptor is more than 10. Therefore, three violations of (1) against Lipinski's rule are tolerated.

The method for delivering of (1) as a drug to overcome the rule of five violations can be in the form of lipid and polymer nanoparticles. Lipid nanoparticles are suitable carriers for loading hydrophilic and lipophilic drugs, which can be used via various routes, including topical, oral, parenteral, ocular, pulmonary, and brain drug delivery. On the other hand, the most important features of polymer-based nanocarriers are the increased stability of the enveloped drug, he ability to deliver higher amounts of the active substance to the target tissue as well as guard the active substance against hydrolysis and enzymatic degradation. Cytotoxicity of nanopolymers as carriers shows that these carriers are not toxic to HeLa cells [38].

The results of the toxicity test using Toxtree program showed that based on the revised Cramer decision tree parameter, (1) is classified as Class II (intermediate). Compounds classified as Class II are less innocuous than Class I (very harmless), but do not contain structures that exhibit the same toxicity as substances in class III (might be toxic or contain reactive functional group). The results of the skin corrosion parameter test showed that (1) does not cause skin irritation or corrosion. The results obtained through the test of genotoxic and nongenotoxic, and mutagenicity parameters showed that (1) is negative for genotoxic and nongenotoxic carcinogenicity. Based on

the results of the toxicity test using three parameters, showed that (1) is non-toxic. Therefore, (1) has the potential to be a SARS-CoV-2 drug candidate.

4. Conclusion

Molecular docking and molecular dynamics simulations of *P. niruri*, *C. xanthorrhiza*, and *O. aristatus* secondary metabolites showed that rutin (1) contained in *P. niruri* leaves has the lowest binding score with S-glycoprotein (6LZG) and $3CL^{pro}$ (6LU7) SARS-CoV-2 than remdesivir and nelfinavir. In its best docking score, (1) formed hydrogen bonds with S-glycoprotein residues that were important for the binding of S-glycoprotein to human ACE2, including TYR449, GLN493, GLN498 and pi-sulfur interaction with $3CL^{pro}$ catalytic point, CYS145. The results of the molecular dynamics simulation showed that the $3CL^{pro}$-(1) complex was stable during the 10 ns simulation. The pharmacokinetic properties and toxicity of (1) indicate this compound is non-toxic and could be used as a drug even though it violates three Lipinski's rules. The synthetic accessibility score of (1) indicates this compound is quite easy to synthesize. Therefore, (1) has the potential to become a SARS-CoV-2 drug.

Acknowledgement

This research was sponsored by the LPDP-BPI scholarship program of the Indonesian government.

References

[1] JOGALEKAR M P, VEERABATHINI A, & GANGADARAN P. Novel 2019 coronavirus: genome structure, clinical trials, and outstanding questions. *Experimental Biology and Medicine*, 2020, 245(11): 964-969. https://doi.org/10.1177/1535370220920540

[2] JAIMES J A, ANDRE N M, CHAPPIE J S, et al. Phylogenetic analysis and structural modelling of SARS-CoV-2 spike protein reveals an evolutionary distinct and proteolytically sensitive activation loop. *Journal of Molecular Biology*, 2020, 432(10): 3309-3325. https://doi.org/10.1016/j.jmb.2020.04.009

[3] GYEBI G A, OGUNRO O B, ADEGUNLOYE A P, et al. Potential inhibitors of coronavirus 3-chymotrypsin-like protease ($3CL^{pro}$): an *in silico* screening of alkaloids and terpenoids from African medicinal plants. *Journal of Biomolecular Structure and Dynamics*, 2021, 39(9): 3396-3408. https://doi.org/10.1080/07391102.2020.1764868

[4] GURUNG A B, ALI M A, LEE J, et al. Unravelling lead antiviral phytochemicals for the inhibition of SARS-CoV-2 M^{pro} enzyme through in silico approach. *Life Sciences*, 2020, 117831: 1-13. https://doi.org/10.1016/j.lfs.2020.117831

[5] ADZKIA A. *COVID-19: Setahun Pandemi Virus Corona, Indonesia Belum Aman Masih Stadium Empat*. BBC East Asia Visual Journalism, 2021. Retrieved from https://www.bbc.com/indonesia/indonesia-56238695).

[6] WHO. COVID-19 Weekly Epidemiological Update, 2021. Retrieved from https://apps.who.int/iris/bitstream/handle/10665/341329/CoV-weekly-sitrep 11May21

[7] WHO. COVID-19 Weekly Epidemiological Update Ed 45, 2021. Retrieved from https://apps.who.int/iris/bitstream/handle/10665/342009/CoV-weekly-sitrep22Jun21

[8] SOHRABI C, ALSAFI Z, O'NEILL N, et al. World Health Organization declares global emergency: A review of the 2019 novel coronavirus (COVID-19). *International Journal of Surgery*, 2020, 76: 71-76. https://doi.org/10.1016/j.ijsu.2020.02.034

[9] PETROSILLO N, VICECONTE G, ERGONUL O, et al. COVID-19, SARS and MERS: are they closely related? *Clinical Microbiology and Infection*, 2020, 26(6): 729-734. https://doi.org/10.1016/j.cmi.2020.03.026

[10] LAKSMIANI N P L, LARASANTY L P F, SANTIKA, et al. Active Compounds Activity from the Medicinal Plants Against SARS-CoV-2 using in Silico Assay. *Biomedical and Pharmacology Journal*, 2020, 13(2): 873-881. http://dx.doi.org/10.13005/bpj/1953

[11] ABDEL-AZEZ AERON A, & KAHIL T A. Health benefits and possible risks of herbal medicine. In GARG N, ABDEL-AZIZ S, & AERON A. (Eds) *Microbes in Food and Health*, 2016: 97-116. https://doi.org/10.1007/978-3-319-25277-3_6.

[12] LIPINSKI C A, LOMBARDO F, DOMINY B W, & FEENEY P J. Experimental and computational approaches to estimate solubility and permeability in drug discovery and development settings. *Advanced Drug Delivery Reviews*, 2012, 64(1-3): 4-17. https://doi.org/10.1016/s0169-409x(00)00129-0

[13] NEVES B J, BRAGA R C, MELO-FILHO C C, et al. QSAR-based virtual screening: advances and applications in drug discovery. *Frontier in Pharmacology*, 2018, 9: 1275. https://doi.org/10.3389/fphar.2018.01275.

[14] PARIKESIT A A, & NURDIANSYAH R. Drug repurposing option for COVID-19 with structural bioinformatics of chemical interactions approach. *Cermin Dunia Kedokteran*, 2020, 47(3): 222-226. https://doi.org/https://dx.doi.org/10.55175/cdk.v47i3.376

[15] TALLEI T E, TUMILAAR S G, NIODE N J, et al. Potential of plant bioactive compounds as SARS-CoV-2 main protease (M^{pro}) and spike (S) glycoprotein inhibitors: a molecular docking study, *Preprints*, 2020, https://doi.org/10.20944/preprints 202004.0102.v3, 1-17.

[16] GOSH R, CHAKRABORTY A, BISWAS A, & CHOWDHURI S. Identification of polyphenols from *Broussonetia papyrifera* as SARS CoV-2 main protease inhibitors using *in silico* docking and molecular dynamics simulation approaches. *Journal of Biomolecular Structure and Dynamics*, 2020, 39(17): 6747-6760. https://doi.org/10.1080/07391102.2020.1802347.

[17] WAHYUNI T S, AZMI D, PERMANASARI, et al. Anti-viral activity of *Phyllantus niruri* against Hepatitis C Virus. *Malaysian Applied Biology*, 2019, 48(3): 105-111.

[18] FARA-TELLO P, MIRAZO S, DUTRA C, et al. Cytotoxic, virucidal, and antiviral activity of South American plant and algae extracts. *The Scientific Journal*, 2012, ID 174837: 1-5. https://doi.org/10.1100/2012/174837

[19] TAN W C, JAGANATH I B, MANIKAM R, & SEKARAN S D. Evaluation of antiviral activities of four local Malaysian Phyllantus species against Herpes Simplex Viruses and possible antiviral target. *International Journal of Medical Sciences*, 2013, 10(13): 1817-1829. https://doi.org/10.7150/ijms.6902

[20] KARYAWATI A T. Aktivitas antivirus Simian

Retrovirus Stereotype-2 (SRV-2) dari ekstrak meniran (Phyllantus niruri) dan Temulawak (Curcuma xanthorrizha), *Jurnal Penelitian Sains*, 2011, 14(3): 52-55. https://doi.org/10.36706/jps.v14i3.216
[21] SYAMSUDIN R A M R, PERDANA F, MUTIAZ, et al. Tanaman temulawak (*C. xanthorrhiza* Roxb) sebagai obat tradisional. *Jurnal Ilmiah Farmako Bahari*, 2019, 10(1): 51-65. https://doi.org/10.52434/jfb.v10i1.648
[22] RIPIM N S M, FAZIL N, IBRAHIM S N K, et al. Antiviral properties of *Orthosiphon stamineus* aqueous extract in herpes simplex virus type 1 infected cells. *Sains Malaysiana*, 2018, 47(8): 1725-1730. https://doi.org/10.17576/jsm-2018-4708-11
[23] ALI A M, MACKEEN M M, EL-SHARKAWY S H, et al. Antiviral and cytotoxic activities of some plants used in Malaysian indigenous medicine. *Pertanika Journal Tropic Agricultural Sciences*, 1996, 19(2), 129-136.
[24] RAHMANINGSIH S. & PUJIASTUTIK H. An *in vitro* and an *in silico* evaluation of the antibacterial activity of the bioactive compounds in Majapahit (*Cressentia cujete* L.) fruit. *Veterinary World*, 2019, 12(12): 1959-1965. https://doi.org/10.14202/vetworld.2019.1959-1965
[25] CHOWDURY P. *In Silico* investigation of phytoconstituents from Indian medicinal herb *Tinospora cardifolia* (giloy) against SARS-CoV-2 (COVID-19) by molecular dynamics approach. *Journal of Biomolecular Struture and Dynamics*, 2020, 39(17): 6792-6809. https://doi.org/10.1080/07391102.2020.1803968.
[26] KUO C J, LIU H G, LO Y K, et al. Individual and common inhibitors of coronavirus and picornavirus main proteases. *Federation of European Biochemical Societies*, 2009, 583(3): 549-555. https://doi.org/10.1016/j.febslet.2008.12.059
[27] LIU C, BOLAND S, SCHOLLE M D, et al. Dual inhibition of SARS-CoV-2 and human rhinovirus with protease inhibitors in clinical development. *Antiviral Research*, 2021, 187(105020): 1-8. https://doi.org/10.1016/j.antiviral.2021.105020
[28] OMRANI M, KESHAVARZ M, EBRAHIMI S N, et al. Potential natural products against respiratory viruses: A persepective to develop anti-COVID-19 disease. *Frontiers in Pharmacology*, 2021, 11: 586933. https://doi.org/10.3389/fphar.2020. 586993/full.
[29] HUGGINS D J, & TIDOR B. Systematic placement of structural water molecules for improved scoring of protein-ligand interactions. *Protein Engineering, Design and Selection*, 2011, 24(10): 777-789. https://doi.org/10.1093/protein/gzr036
[30] LIPPERT T, & RAREY M. Fast automated placement of polar hydrogen atoms in protein ligand complexes. *Journal of Cheminformatics*, 2009, 1(13): 1-12. https://doi.org/10.1186/1758-2946-1-13.
[31] TROTT O, & OLSON J. A. Autodock Vina: improving the speed and accuracy of docking with new scoring function, effiecient optimization and multithreading. *Journal Computational Chemistry*, 2010, 31(2): 455-461. https://doi.org/10.1002/jcc.21334
[32] VARGAS J A R, LOPEZ A G, PINOL M C, & FROEYEN M. Molecular docking study on the interaction between 2-substituted-4,5-difuryl imidazoles with different protein target for antileishmanial activity. *Journal of Applied Pharmaceutical Science*, 2018, 8(3): 14-22. https://doi.org/10.7324/JAPS.2018.8303
[33] ALI A, & VIJAYAN R. Dynamics of the ACE2-SARS-CoV-2/SARS-CoV spike protein interface reveal unique mechanisms. *Scientific Reports*, 2020, 10(1): 14214, 1-12. https://doi.org/10.1038/s41598-020-71188-3.
[34] UL-QAMAR M.T, ALQAHTANI S M, ALAMRI M A, & CHEN L L. Structural basis of SARS-CoV-2 $3CL^{pro}$ and anti-COVID-19 drug discovery from medicinal plants. *Journal of Pharmaceutical Analysis*, 2020, 10(4): 313-319. https://doi.org/10.1016/j.jpha.2020.03.009
[35] JUKIC M, SKRLJ B, TOMSIC G, et al. Prioritisation of compounds for $3CL^{pro}$ inhibitor development on SARS-CoV-2 variants. *Molecules*, 2021, 26(10), 3003: 1-14. https://doi.org/10.3390/molecules26103003
[36] LIN J H. & YAMAZAKI M. Role of P-glycoprotein in pharmacokinetics: clinical implications. *Clinical Phamacokinetics*, 2003, 42(1): 59-98. https://doi.org/10.2165/00003088-200342010-00003.
[37] LIN J H. & LU A Y H. Inhibition and induction of Cytochrome P450 and the clinical implications. *Clinical Pharmacokinetics*, 1998, 35(5): 361-390. https://doi.org/10.2165/00003088-199835050-00003
[38] NEGAHDARI R, BOHLOULI S, SHARIFI S, et al. Therapeutic benefits of rutin and its nanoformulations. *Phytotherapy Research*, 2021, 35(4): 1719-1738. https://doi.org/10.1002/ptr.6904.

参考文:

[1] JOGALEKAR MP P、VEERABATHINI A 和 GANGADARAN P。2019 年新型冠状病毒：基因组结构、临床试验和突出问题。实验生物学与医学，2020, 245(11): 964-969. https://doi.org/10.1177/1535370220920540
[2] JAIMES J A、ANDRE N M、CHAPPIE J S 等。SARS-CoV-2 刺突蛋白的系统发育分析和结构建模揭示了一个进化独特且对蛋白水解敏感的激活环。分子生物学杂志，2020, 432(10): 3309-3325. https://doi.org/10.1016/j.jmb.2020.04.009
[3] GYEBI G A，OGUNRO OB，ADEGUNLOYE AP 等。冠状病毒 3-胰凝乳蛋白酶样蛋白酶(3CLpro)的潜在抑制剂：非洲药用植物中生物碱和萜类化合物的计算机筛选。生物分子结构与动力学杂志, 2021, 39(9): 3396-3408. https://doi.org/10.1080/07391102.2020.1764868
[4] GURUNG A B，ALI MA，LEE J，等。通过计算机模拟方法揭示了用于抑制 SARS-CoV-2 姆普罗酶的先导抗病毒植物化学物质。生命科学，2020，117831：1-13。https://doi.org/10.1016/j.lfs.2020.117831
[5] ADZKIA A. 新冠肺炎：冠状病毒大流行的一年，印度尼西亚仍处于第四阶段并不安全。英国广播公司东亚视觉新闻，2021。摘自 https://www.bbc.com/indonesia/indonesia-56238695）。
[6] 世界卫生组织。2021 年新冠肺炎每周流行病学更新。摘自

https://apps.who.int/iris/bitstream/handle/10665/341329/CoV-weekly-sitrep 11May21

[7] 世界卫生组织。新冠肺炎每周流行病学更新，2021 年第 45 版。摘自 https://apps.who.int/iris/bitstream/handle/10665/342009/CoV-weekly-sitrep22Jun21

[8] SOHRABI C、ALSAFI Z、O'NEILL N 等。世界卫生组织宣布全球进入紧急状态：对 2019 年新型冠状病毒(新冠肺炎)的回顾。国际外科杂志，2020，76：71-76。https://doi.org/10.1016/j.ijsu.2020.02.034

[9] PETROSILLO N、VICECONTE G、ERGONUL O 等。新冠肺炎、非典和中东呼吸综合征：它们密切相关吗？临床微生物学与感染，2020, 26(6): 729-734. https://doi.org/10.1016/j.cmi.2020.03.026

[10] LAKSMIANI N P L、LARASANTY L P F、SANTIKA 等。使用计算机模拟测定药用植物抗 SARS-CoV-2 的活性化合物活性。生物医学与药理学杂志, 2020, 13(2): 873-881. http://dx.doi.org/10.13005/bpj/1953

[11] ABDEL-AZEZ AERON A, 和 KAHIL T A. 草药的健康益处和可能的风险。摘自 GARG N、ABDEL-AZIZ S 和 AERON A.（编辑）《食品与健康中的微生物》，2016：97-116。https://doi.org/10.1007/978-3-319-25277-3_6。

[12] LIPINSKI CA、LOMBARDO F、DOMINY B W 和 FEENEY P J。在药物发现和开发环境中估计溶解度和渗透性的实验和计算方法。高级药物递送评论，2012，64(1-3)：4-17。https://doi.org/10.1016/s0169-409x(00)00129-0

[13] NEVES B J、BRAGA RC、MELO-FILHO CC 等。基于定量 SAR 的虚拟筛选：药物发现的进展和应用。药理学前沿，2018，9：1275。https://doi.org/10.3389/fphar.2018.01275。

[14] PARIKESIT A A, 和 NURDIANSYAH R。采用化学相互作用结构生物信息学方法的新冠肺炎药物再利用选择。医学世界镜报，2020, 47(3): 222-226. https://doi.org/https://dx.doi.org/10.55175/cdk.v47i3.376

[15] TALLEI T E、TUMILAAR S G、NIODE N J 等。植物生物活性化合物作为 SARS-CoV-2 主要蛋白酶(姆普罗)和刺突(S)糖蛋白抑制剂的潜力：分子对接研究，预印本，2020，https://doi.org/10.20944/preprints 202004.0102.v3, 1- 17.

[16] GOSH R、CHAKRABORTY A、BISWAS A 和 CHOWDHURI S。使用计算机对接和分子动力学模拟方法鉴定构树多酚作为 SARS CoV-2 主要蛋白酶抑制剂。生物分子结构与动力学，2020, 39(17): 6747-6760. https://doi.org/10.1080/07391102.2020.1802347。

[17] WAHYUNI TS、AZMI D、PERMANASARI 等。叶下珠对丙型肝炎病毒的抗病毒活性。马来西亚应用生物学, 2019, 48(3): 105-111.

[18] FARA-TELLO P、MIRAZO S、DUTRA C 等。南美植物和藻类提取物的细胞毒性、杀病毒和抗病毒活性。《科学杂志》，2012，ID 174837：1-5。https://doi.org/10.1100/2012/174837

[19] TAN W C、JAGANATH I B、MANIKAM R 和 SEKARAN S D。四种马来西亚当地叶珠属植物对单纯疱疹病毒和可能的抗病毒目标的抗病毒活性评估。国际医学科学杂志，2013，10(13)：1817-1829。https://doi.org/10.7150/ijms.6902

[20] KARYAWATI A T. 来自梅尼兰(珍珠草)和铁木拉越(黄根)提取物的猿猴逆转录病毒刻板型 2 (SRV-2)的抗病毒活性，科学研究杂志，2011, 14(3): 52-55。https://doi.org/10.36706/jps.v14i3.216

[21] SYAMSUDIN R A M R、PERDANA F、MUTIAZ 等。铁木拉越植物（C.黄芪）作为传统药物。海洋药典科学杂志，2019，10(1)：51-65。https://doi.org/10.52434/jfb.v10i1.648

[22] RIPIM N S M、FAZIL N、IBRAHIM S N K 等。雄管管虫水提取物对 1 型单纯疱疹病毒感染细胞的抗病毒特性。《马来西亚科学》，2018，47(8)：1725-1730。https://doi.org/10.17576/jsm-2018-4708-11

[23] ALI A M、MACKEEN MM、EL-SHARKAWY SH 等。一些植物的抗病毒和细胞毒活性被用于马来西亚本土医学。农业杂志热带农业科学，1996, 19(2), 129-136。

[24] RAHMANINGSIH S. 和 PUJIASTUTIK H. 对满者伯夷(库杰特克雷森蒂亚.)果实中生物活性化合物的抗菌活性进行体外和计算机评估。兽医世界，2019，12（12）：1959-1965。https://doi.org/10.14202/vetworld.2019.1959-1965

[25] CHOWDURY P. 通过分子动力学方法对印度药草青牛胆(心叶青牛胆) (吉洛伊)的植物成分进行计算机模拟研究，以对抗 SARS-CoV-2 (新冠肺炎)。生物分子结构与动力学，2020, 39(17): 6792-6809. https://doi.org/10.1080/07391102.2020.1803968。

[26] KUO C J, LIU H G, LO Y K, 等. 冠状病毒和小核糖核酸病毒主要蛋白酶的单独和常见抑制剂。欧洲生化学会联合会，2009，583(3)：549-555。https://doi.org/10.1016/j.febslet.2008.12.059

[27] LIU C，BOLAND S，SCHOLLE MD，等。临床开发中使用蛋白酶抑制剂对 SARS-CoV-2 和人鼻病毒进行

双重抑制。抗病毒研究，2021，187(105020)：1-8。https://doi.org/10.1016/j.antiviral.2021.105020

[28] OMRANI M、KESHAVARZ M、EBRAHIMI S N 等。对抗呼吸道病毒的潜在天然产品：开发抗新冠肺炎疾病的视角。药理学前沿，2021，11：586933。https://doi.org/10.3389/fphar.2020。586993/已满。

[29] HUGGINS D J, 和 TIDOR B. 结构水分子的系统放置，以提高蛋白质-配体相互作用的评分。蛋白质工程设计与选择，2011, 24(10): 777-789. https://doi.org/10.1093/Protein/gzr036

[30] LIPPERT T, 和 RAREY M. 在蛋白质配体复合物中快速自动放置极性氢原子。化学信息学杂志，2009，1(13)：1-12。https://doi.org/10.1186/1758-2946-1-13。

[31] TROTT O, 和 OLSON J. A. 维纳奥托克：通过新的评分功能、高效优化和多线程提高对接速度和准确性。计算化学，2010, 31(2): 455-461. https://doi.org/10.1002/jcc.21334

[32] VARGAS J A R、LOPEZ A G、PINOL MC 和 FROEYEN M。2-取代-4,5-二呋喃基咪唑与不同蛋白质靶标之间相互作用的分子对接研究抗利什曼活性。应用药学杂志，2018, 8(3): 14-22. https://doi.org/10.7324/JAPS.2018.8303

[33] ALI A, 和 VIJAYAN R. ACE2-SARS-CoV-2/SARS-CoV 刺突蛋白界面的动力学揭示了独特的机制。科学报告，2020，10(1)：14214，1-12。https://doi.org/10.1038/s41598-020-71188-3。

[34] UL-QAMAR M T、ALQAHTANI S M、ALAMRI M A 和 CHEN L L。SARS-CoV-2 3CLpro 的结构基础和药用植物中抗新冠肺炎 药物的发现。药物分析杂志，2020，10(4)：313-319。https://doi.org/10.1016/j.jpha.2020.03.009

[35] JUKIC M、SKRLJ B、TOMSIC G 等。优先开发针对 SARS-CoV-2 变体的 3CLpro 抑制剂化合物。分子，2021, 26(10), 3003: 1-14。https://doi.org/10.3390/molecules26103003

[36] LIN J H. 和 YAMAZAKI M. 磷-糖蛋白在药代动力学中的作用：临床意义。临床药代动力学, 2003, 42(1): 59-98. https://doi.org/10.2165/00003088-200342010-00003。

[37] LIN J H. 和 LU A Y H. 细胞色素磷 450 的抑制和诱导及其临床意义。临床药代动力学，1998，35(5)：361-390。https://doi.org/10.2165/00003088-199835050-00003

[38] NEGAHDARI R、BOHLOULI S、SHARIFI S, 等。芦丁及其纳米制剂的治疗功效。植物疗法研究，2021, 35(4): 1719-1738。https://doi.org/10.1002/ptr.6904。